Taylor & Francis
Taylor & Francis Group

REVIEW

🔓 OPEN ACCESS   Check for updates

Optimal site selection and image fusion guidance technology to facilitate cardiac resynchronization therapy

Benjamin J. Sieniewicz[a,b], Justin Gould[a,b], Bradley Porter[a,b], Baldeep S Sidhu[a,b], Jonathan M Behar[a,b], Simon Claridge[a,b], Steve Niederer[a] and Christopher A. Rinaldi[a,b]

[a]Division of Imaging Sciences and Biomedical Engineering, King's College London, London, United Kingdom; [b]Cardiology Department, Guys and St Thomas' NHS Foundation Trust, London, United Kingdom

ABSTRACT

Introduction: Cardiac resynchronization therapy (CRT) has emerged as one of the few effective treatments for heart failure. However, up to 50% of patients derive no benefit. Suboptimal left ventricle (LV) lead position is a potential cause of poor outcomes while targeted lead deployment has been associated with enhanced response rates. Image-fusion guidance systems represent a novel approach to CRT delivery, allowing physicians to both accurately track and target a specific location during LV lead deployment.

Areas covered: This review will provide a comprehensive evaluation of how to define the optimal pacing site. We will evaluate the evidence for delivering targeted LV stimulation at sites displaying favorable viability or advantageous mechanical or electrical properties. Finally, we will evaluate several emerging image-fusion guidance systems which aim to facilitate optimal site selection during CRT.

Expert commentary: Targeted LV lead deployment is associated with reductions in morbidity and mortality. Assessment of tissue characterization and electrical latency are critical and can be achieved in a number of ways. Ultimately, the constraints of coronary sinus anatomy have forced the exploration of novel means of delivering CRT including endocardial pacing which hold promise for the future of CRT delivery.

1. Introduction

One in five people will suffer from heart failure (HF) during their lifetime and once diagnosed, ~40% of patients die within 1 year [1]. Cardiac resynchronization therapy (CRT), by pacing the left (LV) and right (RV) ventricles to re-coordinate cardiac electrical activation and produce a synchronous contraction, has emerged as one of the few effective treatments for HF [2,3]. However, at present 30% of patients fail to respond clinically through improved quality of life, exercise capacity and New York Heart Association (NYHA) functional classification of HF and up to 50% show no beneficial changes in cardiac function [3]. Suboptimal LV lead position is a common culprit when evaluating poor outcomes after CRT [4–7]. Equally, several groups have reported enhanced response rates when targeting tissue which displays evidence of favorable viability [8–11] or advantageous mechanical [12–18] or electrical [19–23] properties. This review will evaluate how to define the optimal LV pacing site and the mechanisms by which it is possible to selectively deploy a pacing electrode at this site.

2. Acute and chronic markers of response

In order to identify the optimal pacing location, it is necessary to perform an examination of the available sites and preferentially select the site which possesses the most favorable characteristics. Unfortunately, in the 20 years since the first description of resynchronization pacing for HF [24], no consensus has been achieved on how to define 'response' to CRT [25] making comparison of the various pacing sites problematic. A multitude of different clinical and event-based definitions of response to CRT have been described with rates of response varying from 32% to 91% depending on the criteria used. This review will predominantly focus on three indices; outcome-based metrics which evaluate survival and mortality after device implantation. Markers of left ventricular reverse remodeling (LVRR) following device implantation, of which a reduction in LV end-systolic volume (LVESV) is the most widely accepted marker [26,27]. Finally, some metrics evaluate acute changes in LV contractility. Acute hemodynamic response (AHR) is a reproducible marker of LV contractility best expressed as the change in the maximum rate of left ventricular pressure ($LV\text{-}dP/dt_{max}$), from a baseline control state [28,29]. Previous work has evaluated the acute hemodynamic effects of CRT using $LV\text{-}dP/dt_{max}$ as an outcome measure [29–32], and this metric has been used to compare the effects of biventricular (BiV) pacing at different locations [28,29,33]. An improvement in LV-dP/

dt_{max} of 10% during acute implantation has been shown to predict chronic LV reverse remodeling in patients receiving CRT [34].

3. Tissue characterization

3.1. Pathophysiology of scar in ischemic and non-ischemic cardiomyopathy

Ischaemic scar forms as a result of permanent myocyte death following an ischaemic insult. A reparative process is initiated to rebuild the infarcted myocardium and maintain the structural integrity of the ventricle. An initial inflammatory phase of healing is followed by a fibrogenic phase that eventually results in the formation of scar tissue as dead myocytes are progressively replaced by collagenous scar. Ischaemic scar tends to display a sub-endocardial or transmural distribution affecting a specific coronary territory. Histological evidence of myocardial fibrosis has also been described in non-ischaemic presentations [35–37]. While the precise mechanism behind this scar formation, which typically follows an epicardial or mid-will distribution, is unclear, interstitial and perivascular fibrosis ultimately results in myocardial necrosis [38].

3.2. Impact of scar on the mechanical properties of the heart

Almost immediately following coronary artery occlusion, the subtended area of myocardium becomes passive and non-contractile. The non-viability and reduced plasticity of infarcted scar tissue is associated with a reduction in efficient and effective mechanical function during systole. Nearly all of the determinants of systolic function are negatively impacted by the presence of scar including cardiac shape and dimensions, preload, afterload and contractility [39]. During systole, the scared region stretches and bulges outward while the remaining myocardium contracts, causing a reduction in the mechanical efficiency of the heart as a pump. This effect is strongly dependent on the total area of scared tissue [40].

3.3. Impact of scar on outcomes

The size, location, and transmurality of scar all impact LV remodeling after CRT. Global scar burden has been shown to be inversely proportional to LV reverse remodeling amongst both ischemics [41], non-ischemics [42], and mixed populations [43–45]. Functional improvement [41,42,46] and survival [47] are also inversely proportional to scar burden. Retrospective analysis has confirmed that favorable markers for response include smaller scar size and fewer areas of transmural scar [45]. The location of scar is of equal importance, in particular when it is located in the posterolateral region of the LV, a site empirically thought to be optimal for LV lead deployment. Scar in this area is associated with lower response rates following CRT [45,48].

3.4. Impact of scar on electrical activation

Scar prevents effective transmission of the electrical impulse, resulting in prolonged activation. Electrical activation in regions of fibrosis is characterized by localized delays and fractionated, low-amplitude extracellular electrograms [49]. This has been attributed to changes in patterns of excitation and conduction due to altered ion channel activity [50] and decreased cellular connectivity [51] compounded by tortuous conduction through areas of surviving myocytes. This delay in LV activation results in less hemodynamic improvement during BiV pacing [52]. Electrical stimulation in regions of scar can also be pro-arrhythmic [53,54] and is associated with increased morbidity and mortality [8,55]. Unsurprisingly, the presence of myocardial scar at the site of LV stimulation during CRT is associated with non-response [8,56].

3.5. Scar identification

Given the negative implications associated with stimulating scared and fibrotic myocardial tissue, current evidence favors avoiding these areas and targeting viable tissue. Numerous mechanisms have been proposed in order to differentiate non-viable tissue, and these can be categorized into anatomical, functional, and biological modalities, see Table 1. Anatomical imaging involves direct visualization of tissue defined as scarred. Functional imaging relies on surrogate markers of scar such as measures of wall motion, strain, voltage, or contractile reserve. Biological imaging assesses metabolism or perfusion as a surrogate for viability.

3.6. Cardiac MRI

Late gadolinium enhancement (LGE) cardiac MRI (CMR) is the gold standard for delineating myocardial scar with high resolution, as the superior spatial resolution of LGE-CMR permits differentiation between epicardial, transmural, and sub-endocardial infarction. The technique relies on the fact that gadolinium washes out of the blood pool but accumulates in the extracellular space. Tissues with weak intracellular bonds and high amounts of non-cellular space, including necrotic tissue or fibrous scar, will develop higher concentrations of gadolinium than the surrounding healthy tissues. Scar detected by LGE-CMR has been shown to closely match histologically proven myocardial infarction [57].

3.7. Trans-thoracic echocardiography

Transthoracic echocardiography has the potential to identify areas of scarred or fibrotic myocardium. Early work focused on regional wall thinning [58] and assessment of regional contractile function [59], while more recent work has focused on the ability of speckle-tracking radial strain [60] and longitudinal strain [61] to better identify areas of regional akinesis. Other techniques include the use of 3D contrast echo [62]

Table 1. Techniques for assessment of viability and scar.

Imaging technique	Classification	Technique	Marker of viability/scar
CMR	Anatomical imaging	LGE	Direct visualization of scar
	Anatomical imaging	Wall thickness	EDWT as surrogate for scar
	Functional imaging	Contractile reserve	Contractile reserve
	Functional imaging	Functional assessment	Severe dysfunction as surrogate for scar
	Functional imaging	Strain assessment	Severely reduced strain as surrogate marker
TTE	Anatomical imaging	Wall thickness	EDWT as surrogate for scar
	Functional imaging	Contractile Reserve	Contractile reserve
	Functional imaging	Functional assessment	Severe dysfunction as surrogate for scar
	Functional imaging	Strain assessment	Severely reduced strain as surrogate marker
CT	Anatomical imaging	Wall thickess	EDWT as surrogate for scar
PET or SPECT	Biological imaging	Perfusion	Perfusion as a surrogate for viability
PET or SPECT with FDG	Biological imaging	Glucose utilization	Glucose utilization as a surrogate for viability

CMR: cardiac MRI; LGE: late gadolinium enhancement; CT: computed tomography; PET: positron emission tomography; SPECT: single-photon emission computed tomography; FDG: Fluorine-18-labeled deoxyglucose.

and pulse cancelation echocardiography [63], which have both shown some promise as tools to identify areas of scar.

3.8. Cardiac computed tomography (CT)

Tissue characterization using cardiac CT has been used to identify areas of myocardial scarring. After an infarct, myocardial tissue replaced by fibrous scar and eventually, after several months, undergoes significant lipomatous metaplasia [64]. Using unenhanced CT, it is possible to identify the fat in infarcted myocardium. New-generation dual-source CT (DSCT) allows the integration of late-iodine enhancement imaging and has been shown to correlate reasonably well (52% sensitivity, 88% specificity) with LGE-derived CMR imaging [65].

3.9. Nuclear imaging

Tracer uptake during Nuclear imaging using either positron emission tomography (PET) or single-photon emission CT (SPECT) relies on adequate myocardial blood flow and myocyte viability. The finding of a fixed perfusion defect can either represent myocardial scar or viable hibernating myocardium. Differentiation between these two states can be further enhanced through an assessment of glucose uptake via Fluorine-18-labeled deoxyglucose (FDG) with hypocontractile regions exhibiting reduced perfusion but normal or increased FDG uptake representing likely hibernating myocardium. During head-to-head comparison, MIBI has been shown to consistently overestimate areas of myocardial scar tissue, while FDG lacks the spatial resolution associated with LGE-CMR [66].

3.10. Electroanatomical mapping

While LGE-CMR has the capacity to directly visualize anatomic myocardial scar, the abnormal electrophysiological substrate extends beyond the dense anatomical scar, into regions of heterogeneous 'boarder-zone' tissue [67], and may be optimally identified using electroanatomic mapping (EAM). The ability of EAM to assess myocardial viability on the basis of myocardial voltage has been validated against SPECT [68], PET imaging [69], and latterly LGE-CMR [70–73] in both ischemic

and non-ischemic cardiomyopathies. Furthermore, analysis of electrogram characteristics can also help to predict histologic properties of scar tissue [49].

3.11. Invasive electroanatomical mapping

During invasive EAM, intracardiac electrical activation is recorded in relation to anatomic locations in a particular cardiac chamber of interest, allowing the definition of 3D cardiac chamber geometry as well as delineating areas of anatomic interest such as regions of scar. Systems can be divided into contact and non-contact mapping systems. Contact mapping systems rely on recording local activation between two poles on a mapping catheter. The resulting bipolar voltage map can be thresholded to reveal areas with a voltage outside of normal range for ventricular tissue, typically 0.5 mV to 1.5 mV.

Non-contact mapping systems utilize a multi-electrode array (MEA) catheter to simultaneously record endocardial activation over multiple areas [74]. The array is situated on a balloon with 64 electrodes allowing high-density mapping from a single heartbeat. Advantages of this system include the ability to acquire multiple endocardial electrograms during a single cardiac cycle; however, this comes at the cost of greater inaccuracy in electrogram timing and morphology at greater distances from the MEA [75]. Work evaluating this system has already established that non-contact mapping can identify regions of electrically viable myocardium, which could be used to inform lead position, particularly among ischemic patients [52].

3.12. Electrocardiographic imaging

Electrocardiographic imaging (ECGI) is a novel, non-invasive 3D epicardial electrophysiology imaging modality. This technique uses 252 ECG electrodes mounted on a wearable vest to reconstruct epicardial potentials from torso potentials, see Figure 1. These are displayed as electrograms and activation sequences (isochrones) on the epicardial surface of the heart [76].

ECGI benefits from a non-invasive approach and is able to measure the activation across the whole heart simultaneously compared to the slower sequential mapping with EAM. Inverse ECG mapping technology is able to identify fibrotic

Figure 1. The 252-lead vest records torso surface electrograms. Reproduced with permission from MEDTRONIC.

tissue due to the abnormal electrical properties exhibited by scarred myocardium, specifically low-amplitude electrical potentials with broad fractionated electrograms typically in areas exhibiting delayed or slow activation [77–79]. A degree of discrepancy between CMR and EAM is expected as CMR can struggle to detect areas of homogenous microscopic diffuse fibrosis due to the low resolution of the image, while inverse ECG EAM can be more sensitive at detecting zones of epicardial and transmural fibrosis but may miss sub-endocardial scar. Despite this, good correlation has been observed between areas of low voltage on ECGI and areas of scar, as identified on LGE-CMR [80] with one study quoting an 89% sensitivity and 85% specificity at detecting epicardial scar [81].

4. Dyssynchrony assessment and identification of the site of latest mechanical activation (LMA)

A paradox exists between the electrical substrate corrected by CRT, specifically dyssynchronous BiV electrical activation and its mode of action, which is predominately mechanical and aims to enhance cardiac contractility by correcting the mechanical dyssynchrony and restoring the mechano-energetic efficiency of the heart. Intuitively, it would seem sensible to specifically assess the degree of mechanical dyssynchrony present, as this would both help patient selection and aid in the determination of the optimal LV pacing site. Dyssynchrony is the measure of dispersion in the timing of mechanical contraction of the various LV segments [82] and may be measured by a variety of different imaging techniques.

4.1. Transthoracic echocardiography

Early work assessing the utility of echocardiographic parameters of dyssynchrony to aid patient selection for CRT appeared promising. A systolic dyssynchrony index (SDI), calculated from tissue Doppler imaging (TDI), proved capable of retrospectively predicting enhanced clinical response in single-center work [83]. These benefits were also observed in a multicenter retrospective analysis where the use of baseline TDI imaging predicted not only functional and echocardiographic improvement but also identified patients who yielded prognostic benefit from CRT [84]. Speckle-tracking radial strain analysis superseded TDI, as it was less dependent on the angle of incidence of the ultrasound beam and also appeared able to predict echocardiographic response in retrospective analysis [85].

Unfortunately, the utility of mechanical dyssynchrony assessment to identify CRT responders has not been reproduced in larger, prospective, randomized multicenter studies [86] and this has cast some doubt on the reproducibility of the technique. In addition, when all the various echocardiographic measures of mechanical dyssynchrony were analyzed in a large, international multicenter study, no single measure proved capable of improving patient selection for CRT [87]. Promisingly, newer techniques including longitudinal myocardial strain assessment [88] and 3D speckle-tracking echo [89] appear more reliable and indicate an encouraging direction for future work.

Given the primary target of CRT is the restoration of coordinated myocardial contraction and those patients exhibiting mechanical dyssynchrony appeared to yield the most benefit from CRT, it seemed logical that the optimal site for LV lead deployment would be at the site of maximal mechanical delay. In a retrospective analysis where TDI assessment of mechanical activation was performed prior to CRT implantation, patients in whom the LV lead was situated at the site exhibiting the latest activation showed increased functional and echocardiographic improvements [15]. Superior response to CRT was also observed when the site of LMA was targeted using tissue synchronization imaging (TSI) [90], 3D echocardiography [91], and speckle tracking [92]. The TARGET [13] and STARTER [16] trials prospectively assessed the utility of echocardiographic speckle-tracking two-dimensional radial strain imaging to inform LV lead deployment. Echo-guided lead

implantation was associated with echocardiographic response rates (>15% reduction in ESV) of 70% and 57%, respectively. Both studies showed increased rates of event-free survival over empirical lead placement.

4.2. Cardiac MRI

CMR has several potential advantages when looking to characterize mechanical activation. These include greater reproducibility, less artifact secondary to patient habitus, detailed assessment of myocardial tissue characterization as well as chamber size, and volumes and greater spatial resolution. CMR can also assess strain in multiple planes allowing the assessment of both radial and longitudinal strain. A recent prospective, single-center randomized study (CMR-CRT) showed the feasibility of performing an assessment of circumferential strain in order to identify the latest mechanically activated viable segment [93]. Several dyssynchrony assessment metrics have been proposed including myocardial tagging, displacement encoding with stimulated echoes, and phase contrast tissue velocity mapping. While myocardial tag data has been shown to predict functional improvement following CRT implantation [94], tag decay remains an issue and this led to the development of 3D volumetric change as a means of assessing both global LV dyssynchrony and assessing mechanical activation [95]. When compared to other mechanical dyssynchrony measures, volume changeSDI proved the sole predictor of chronic reverse remodeling [18].

4.3. Cardiac CT

Cardiac CT offers a potential benefit over CMR due to the fact that approximately 28% of patients undergoing CRT implantation have already received an implantable cardiac device rendering them unsuitable to undergo CMR scanning [96]. Cardiac CT is associated with submillimeter spatial resolution and can assess regional and global LV dyssynchrony by calculating the stretch of the endocardial surface throughout the cardiac cycle (stretch quantifier for endocardial engraved zones [SQUEEZ]) [97]. When assessed in patients undergoing an upgrade to a CRT pacing system, CT-SQUEEZ targets were associated with a similar improvement in AHR as the best achievable (20.4% ± 13.7% vs. 24.9% ± 11.1%; $P = 0.36$) [98]. In addition, delivering LV stimulation at a site identified using CT-SQUEEZ resulted in greater clinical response vs. non-target segments (90% vs. 60%, $P < 0.001$).

5. Identifying the site of latest electrical activation (LEA)

The primary substrate targeted during CRT is delayed electrical activation, typically manifest by a left bundle branch block (LBBB) pattern on the surface ECG. Detailed analysis of ventricular activation confirms a myriad of differing underlying conduction disturbances amongst even this group, with ischemic patients displaying a particularly high degree of variability in activation [99]. The standard 12 lead ECG is therefore of limited use when looking to define the optimal site for LV stimulation, and focus has shifted to more detailed methods of visualizing

electrical latency. In the context of LBBB, ventricular activation is initiated at the distal branching of the right bundle, with activation of the left endocardium occurring after a significant delay, as a result of slow conduction through the interventricular septum. Theoretically, the site of latest activation should exhibit the most dyssynchrony and as such would represent an ideal pacing site. While some work appears to confirm the site of LEA is synonymous with the optimal pacing site [21], more recent analysis has shown optimal site exhibits late but not supremely delayed activation [100]. Sites demonstrating excessively delayed activity may in fact merely represent distal activation occurring within islands of non-viable tissue. A variety of different methods of identifying the site of latest activation have been described, as outlined below.

5.1. Q-LV and LV lead electrical delay

An advantage of assessing electrical delay is that it can be performed both intra-procedurally and without the need for any additional mapping equipment. Singh et al., devised a measure of electrical latency called the left ventricular lead electrical delay (LVLED) [20]. This marker of electrical delay was calculated during LV lead implantation by determining the onset of the surface ECG-QRS complex to the onset of the sensed electrogram on the LV lead and expressing the value (the Q-LV time) as a percentage of the baseline QRS interval. They identified that LVLED correlated with greater hemodynamic improvements (derived using transthoracic echo).

When dichotomized, patients with an LVLED of >50% exhibited greater event-free survival and reduced rates of hospitalization. In a sub-study of the SMART AV trial [101], patients were again dichotomized, although this time according to the median Q-LV value (95 ms). Gold et al. showed that implanting the LV lead at a site with a favorable Q-LV was independently associated with symptomatic improvement and greater reverse remodeling at 6 months [19].

Both of these studies retrospectively analyzed the degree of electrical latency at the site of LV lead deployment; however, Zanon et al. evaluated whether Q-LV might be used to identify the optimal site in an individual patient by systematically screening all of the suitable coronary sinus (CS) veins [21]. A strong correlation was observed between Q-LV prolongation and improvements in acute hemodynamic response. Again a Q-LV value of greater than 95 ms appeared significant, yielding an improvement in AHR of >10%, a finding which has been associated with predicting long-term remodeling [34]. Crucially, in 96.8% of patients, the optimal hemodynamic performance was associated with delivering pacing therapy at the site exhibiting the LEA. A similar figure (85%) was observed by van Gelder et al. in their evaluation of the effects of LV endocardial pacing amongst a cohort of non-responders to epicardial CRT [102]. The small discrepancy may be attributed to the larger cohort of ischemic patients in this study.

5.2. Narrowing of the paced QRS

Reductions in the paced QRS duration (QRSd) during BiV pacing may also aid identification of late activating tissue.

Widening of the QRS after CRT implantation has been found to be an independent predictor of mortality or progression to heart transplantation[103], and achieving a reduction in the paced QRS has been shown to predict response in several studies [104] including via multivariate logistic regression [105]. In other work, a reduction in paced QRSd was found to be the only predictor of response [106]. However, this finding is disputed in other studies [107]. There is also no consensus as to whether delivering BiV pacing at a site which achieves a narrowing of the paced QRS is associated with improvements in hemodynamics. While some work has shown a correlation between narrowing of the QRS and improvements in AHR [100], this finding has not been consistently replicated [21].

5.3. Invasive electroanatomical mapping

Electroanatomical mapping has also been used to evaluate electrical activation and locate the site of LEA. Analysis of contact and non-contact mapping first data identified a 'U-shaped' pattern of activation during LBBB with depolarization originating at a single septal breakthrough site [99]. Activation could not proceed directly from the anterior to the lateral wall, due to the presence of lines of block, forcing the depolarization wave front to pass inferiorly around the apex. Crucially, even amongst patients who presented with LBBB on their surface ECG, the location of this line of block varied between patients, exposing the heterogeneity of this complex conduction disorder and the difficulty in establishing a universal site of LEA.

More detailed analysis of LV activation revealed heterogeneity in conduction velocities in both non-ischemic and ischemic patients at the site of LV stimulation in the lateral and posterolateral walls [52]. The location of these areas of slow conduction influenced the pattern and direction of wave front propagation. While it was possible to mitigate the effects of positioning the lead in an area of slow conduction by altering the timing between LV and RV stimulation during CRT, locating and stimulating healthy, late-activating tissue was consistently associated with superior hemodynamic improvements.

The anatomical constraints of transvenous, epicardial CRT mean that LV stimulation can only occur at a site accessible via a tributary of the CS. Coronary venous electroanatomical mapping allows the assessment of electrical latency exclusively within the CS [23]. A high degree of variability in the location of the site of LEA was observed between patients. Intra-procedural assessment of latency utilizing this technique is feasible and, while of practical value to the implanting physician, is limited to only those sites accessible via the available coronary venous system.

5.4. Non-invasive electroanatomical mapping of electrical activation

The heterogeneous nature of LV activation in patients with LBBB has also been described using ECGI. A key advantage of this technique is the ability to non-invasively identify the area of LEA, and this approach has already been shown to allow peri-procedural guidance of the LV lead to the target site. ECGI can also compute an LV electrical dyssynchrony index, and this metric appears may predict patients likely to respond to CRT and aid in identifying the optimal site during LV lead deployment [108,109].

5.5. Correlation between the site of LMA and LEA

One hypothesis advanced to explain the persistent issue of non-response to CRT is the existence of uncoupling of mechanical and electrical synchronicity. While these two substrates can be assessed individually, performing an assessment of both may be preferable. Early work appeared to suggest that the site of LEA was synonymous with the area of LMA, when evaluated using non-contact EAM and TTE TDI [110]. Similar findings were observed when the LMA was assessed using CMR [111]. One explanation for this uniformity may be the crucial role played by etiology and the disruptive effects of tissue heterogeneity. The impact of etiology was better assessed by Fujiwara et al. who included patients with both ischemic and non-ischemic cardiomyopathy in their study and identified a clear discrepancy between the site of LMA and LEA [112], see Figure 2. Unanimity between the LMA and the LEA site was only observed in 19% of patients.

5.6. Electrical activation during RV pacing and LBBB

Current class 1 indications for CRT include evidence of dyssynchronous electrical activation, manifest on the surface ECG by
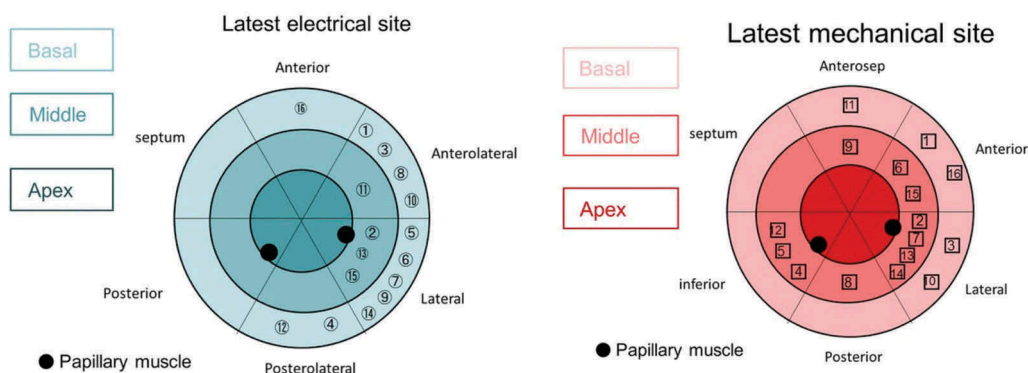

Figure 2. Comparison of sites of LEA (A) and LMA (B). The circled numbers refer to the patient numbers. Reproduced with permission from Wiley.

LBBB. While there has been a great deal of focus on characterizing the precise nature of LV depolarization which occurs during LBBB, activation during CRT occurs as a result of paced stimulation at the LV and typically, the RV apex. While an RV paced event appears morphologically similar on the surface ECG to conduction resulting from LBBB, Eschalier et al. set out to perform a more detailed examination. Non-invasive body surface mapping demonstrated clear differences in the depolarization pattern of both the RV and LV during RV pacing and LBBB activation. Apical pacing resulted in slower RV conduction with lines of conduction detected around the pacing site [113]. LV depolarization was also observed to be prolonged by RV pacing although lines of slow conduction were fewer and shorter in size in comparison to those observed during LBBB activation. The LV site of LEA was similar during both RV apical pacing and LBBB activation and was consistently located at the LV base.

5.7. Electrical activation and RV pacing site selection

RV pacing appears to result in delayed LV depolarization and the deleterious effects of RV apical pacing have been widely acknowledged [114,115]. Positioning the RV lead in a septal position has been associated with beneficial hemodynamic effects [116]. Early work evaluating non-apical RV pacing conducted by Khan et al. [117] showed that LV remodeling rates were unaffected by RV lead position, while Kutyifa et al. [118] also highlighted a higher risk of ventricular arrhythmias. The SEPTAL CRT study randomly assigned patients to receive either a septal or apical RV lead and demonstrated no significant difference in clinical outcome [119].

It is worth noting that there is little consensus on a universal optimal site of LV lead deployment and instead, an individualized approach which takes into account etiology, tissue characterization, and the underlying electrical substrate appears to yield the greatest benefit [120]. Similarly, patient-specific RV lead placement may represent a superior strategy, particularly when faced with limited viable LV pacing sites due to the anatomical constraints associated with transvenous, epicardial CRT. In a pilot study of seven patients, Kumar et al. observed that patient-specific RV lead placement guided by real-time assessment of the cardiac output resulted in significant acute hemodynamic improvements [121].

Electrical latency appears a useful marker when looking to identify the optimal LV pacing site [19,20], and a similar approach can also be used when looking to optimize RV lead position. In the INTER-V study, the measurement of paced RV-LV interlead electrical delay predicted mid-term CRT response [122]. In a blinded, randomized controlled trial which prospectively allocated patients to receive CRT with either RV apical pacing or RV pacing at a site guided by maximal electrical separation (MES), individualized RV lead placement was associated with increased rates of echocardiographic response [123].

6. Site selection during LV-only pacing

LV-only pacing has also been proposed to avoid the negative sequelae associated with RV pacing by preserving intrinsic conduction via the right bundle branch. Different approaches to LV-only pacing have been assessed for both epicardial and endocardial CRT.

6.1. LV-only epicardial pacing

Several comparative studies assessing LV-only epicardial (LV$_{EPI}$) pacing timed to coincide with intrinsic RV activation have been performed. LV$_{EPI}$ pacing has been shown to be associated with non-inferior outcomes [124–126], with some studies showing trends towards superior LV remodeling [127] and improvements in left ventricular ejection fraction [128]. In all these studies, the LV lead was empirically placed in a lateral or posterolateral target vein and as suchit is impossible to predict the implications of delivering LV$_{EPI}$ pacing at an alternative site.

6.2. LV-only endocardial pacing

LV-only endocardial (LV$_{ENDO}$) pacing has also been investigated. The activation of the LV endocardium during CRT is associated with a reduction in both LV and BiV activation time [129]. This is in part explained by the shorter activation path length but also earlier activation of fast-conducting endocardial tissue, which possesses a higher conduction velocity. LV$_{ENDO}$ pacing was associated with greater improvements in AHR than could be achieved using conventional, transvenous CRT (BiV$_{EPI}$) [130]. Only BiV endocardial CRT (BiV$_{ENDO}$) proved capable of yielding a similar hemodynamic improvement.

Much attention has been traditionally focused on correcting the underlying electromechanical delay associated with LBBB by delivering LV stimulation at the site of latest activation, typically identified in the posterolateral wall. An alternative approach is to try and replicate the activation sequence observed during normal sinus rhythm, where activation occurs initially at the left mid-septal endocardium [131,132]. When assessed, activation at this site results in an almost identical temporospatial activation envelope to that observed during normal sinus rhythm, especially when compared to BiV$_{EPI}$, LV$_{EPI}$, and RV$_{ENDO}$ pacing [133]. This can be achieved via a transvenous approach, using a bespoke delivery mechanism incorporating a custom pacing lead which is introduced transvenously into the RV and positioned against the RV septum, before being deployed through the interventricular septum until the left ventricular septum is reached but without perforating the LV septum [134]. One major benefit of this approach is it negates the need for long-term anticoagulation, typically associated with lead-based LV$_{ENDO}$ pacing.

LV$_{ENDO}$ septal pacing can achieve a hemodynamic performance similar to that observed during normal sinus rhythm in patients with preserved LV function [134]. The effects of LV$_{ENDO}$ septal pacing have also been assessed in a small series of patients who fulfill the current criteria for CRT implantation. A combination of RV$_{ENDO}$ and LV$_{ENDO}$ septal pacing achieved the greatest improvement in cardiac stroke work, suggesting that while the septum may represent a potential location to deliver stimulation in patients with impaired LV function, LV$_{ENDO}$ septal pacing alone may not be sufficient to achieve optimal resynchronization [135].

7. Multi-modality imaging and image fusion technology

7.1. Multi-modality imaging

A novel approach to site selection incorporates the fusion of two differing imaging modalities via multi-modality imaging in order to maximize the reliability of the acquisition. Bertini et al. describe an excellent approach aimed at targeting late mechanically activating, viable tissue [136]. Patients first underwent a CMR scan where areas of the myocardial wall displaying of >75% LGE were excluded. The next stage of the 'CRT Team' approach involved the use of 2D speckle-tracking echocardiography which assessed global LV longitudinal strain in order to highlight the most delayed area between non-fibrotic segments. The highest frequency of reverse remodelling at six months (93.1%) was observed in the 58% of patients where the final lead position was concordant with the pre-specified optimal site [136].

Another novel approach employs the fusion of pre-procedural CMR imaging with computer modeling to predict the optimal pacing site. In this series, a 3D navigation model was designed to rank the available sites for LV and RV lead deployment. Sites were graded to ensure the LV lead was directed into the segment with the lowest scar burden which exhibited the greatest mechanical delay while also maximizing the geographic distance between the LV and RV pacing sites. The RC lead tip was directed to the area with the lowest scar burden. The optimal location for the RV lead tip was assigned first followed by the preferential LV pacing site. At follow-up, 74% of patients met the predefined echocardiographic criteria of a responder despite the fact that lead implantation was informed purely by fluoroscopy and visual assessment of the 3D models, and real-time guidance was used [137].

7.2. Image fusion and guidance technology

Optimal site selection can only be achieved when used in conjunction with a targeting system which can identify and inform pacing electrode deployment in real time during implantation. The use of fluoroscopy alone to facilitate targeted electrode deployment is challenging given the radiolucency of the cardiac silhouette and high variability in the rotation of the left and right sided chambers relative to one another. When previously evaluated, concordance between final fluoroscopic LV lead position and CT images was only observed in 35% of patients [138]. In over half of the cases studied, LV lead deployment had actually occurred in an adjacent segment, although this is hardly surprising given the relatively small size of an individual myocardial segment (order of magnitude, cms). As such, site selection and X-Ray co-registration are essential in order to ensure optimal electrode deployment.

7.3. Image fusion with fluoroscopic CS balloon venography

Both the TARGET and STARTER studies showed the benefits of targeting lead deployment at the site of LMA, defined using TTE [13,16]. Unfortunately, in the STARTER study, it was only possible to deploy the lead at the target segment in 30% of patients due to issues with coronary venous anatomy and lead stability. Even in recent work where CMR was used to define the optimal pacing site, concordant LV lead positioning was only achieved in 52% of cases [93]. One approach to facilitate site selection at an achievable location subtended by a tributary of the CS is to evaluate both mechanical activation and CS anatomy. This can be achieved by fusing TTE-derived 3D echo data with fluoroscopic CS balloon venography [14]. Use of this image guidance tool resulted in an LV reverse remodeling rate of 81% of patients, where concordance between final LV lead position and the site of LMA was confirmed. While the use of coronary venous anatomy helps pre-procedural planning, this data was acquired via an additional invasive catheter study.

A more streamlined approach fusing peri-procedural fluoroscopic CS balloon venography with CMR imaging has also been developed [139], see Figure 3(a). A major benefit of this system is the integrated nature of the GuideCRT platform (Siemens Healthineers, Erlangen, Germany). Image processing is automatic with manual verification. A quantitative analysis of LGE is exported including information on scar location, burden, and transmurality. In addition, regional motion analysis of volume vs. time is plotted via endocardial tracking for each of the 16 myocardial segments, allowing identification of the latest activating region, see Figure 3(b). Image processing has now been accelerated to the stage (25 ± 8 min) that the patient can undergo a CMR immediately prior to their CRT implant, and by the time CS venography has been performed, image co-registration can be performed without delay.

Nuclear perfusion imaging can also usefully delineate areas of viable (non-scared) myocardium which display late activation [140]. Again as coronary venous anatomy is not delineated on SPECT imaging, geometric alignment, landmark-based registration, and vessel-surface overlay were used to fuse the 3D venous anatomy with the epicardial mesh derived from the SPECT images [141], see Figure 4.

7.4. Image fusion and guidance technology incorporating CT-derived CS venography

While it is possible to visualize the CS using CMR [142], direct imaging of the sub-branches can be difficult to consistently achieve. CT, however, is capable of accurately delineating the coronary venous tree with submillimeter spatial resolution via rapid acquisition, 3D, isotropic, whole heart data sets [143]. Co-registration between pre-procedural CT-derived volumetric data sets and intra-operative 2D image acquisitions is more straightforward and can be performed using both a feature-based and an intensity-based method [144]. Work evaluating the use of DSCT to both informs site selection and identifies an overlying tributary of the contrary sinus subtending this area is currently ongoing [145], see Figure 5.

8. Expert commentary

Transvenous, epicardial CRT remains the optimal therapy for those patients who exhibit a remediable underlying substrate and whose anatomy is amenable to allow adequate
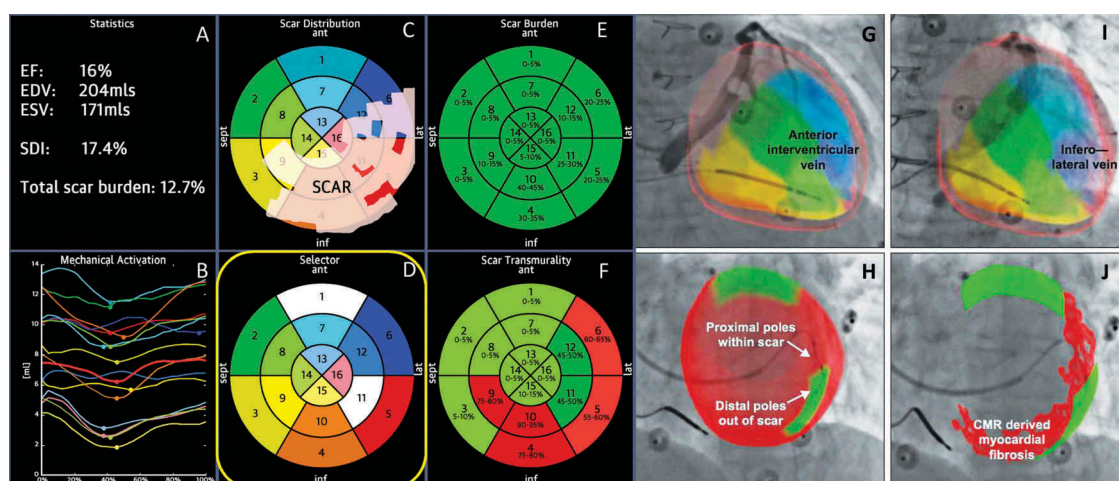
Figure 3. (A) (Top left) Anteroposterior venogram with overlay of CMR-derived epicardial/endocardial shell with 16-segment American Heart Association model showing an anterior interventricular vein. The 3D CMR-derived shell has the same colors as displayed in the guidance platform as shown in Figures 2 and 3. Infero-septal, antero-septal, and anterior segments are colored in yellow, green, and blue, respectively. (Top right) left anterior oblique (LAO) 20 venogram with automated rotation and alignment of the 16-segment model with the x-ray. Inferolateral veins are demonstrated. (Bottom left) LAO 40 projection. The positioning of a quadripolar left ventricular lead into a preselected target segment (green). (Bottom right) LAO 40 projection, alternate view with CMR-derived scar distribution (red). Attempted positioning and pacing using left ventricular poles out of regions of scar. Reproduced with permission from Elsevier due to the creative commons license. (B) This display screen is seen following the processing of the CMR data set and is mimicked on the large screen in the catheter laboratory. Total scar burden calculated as a mean of all myocardial segments. (Top middle) Scar distribution denoted in grey upon an American Heart Association 16-segment model. (Top right) Scar burden (% scar per myocardial segment volume), displayed in 5% ranges. (Bottom right) Scar transmurality demonstrating the mean transmurality from endocardium to epicardium. Those segments >50% transmural myocardial fibrosis are also denoted in red. (Bottom left) Mechanical activation curves for the 16 segments, corresponding to the colors shown in the middle panels. Endocardial tracking of the left ventricle provides absolute changes in the volume per segment (ml, y axis) over the cardiac cycle (0% end diastole, 30% to 50% end systole, 100% end diastole). Because these are absolute volume changes, the apical segments are always at the bottom because they have a smaller start and end volume. When the user hovers over a segment in the top middle panel, the associated volume time curve appears in bold; in this case, the target posterolateral segment is shown. (Bottom middle) Target selection panel. Upon reviewing the scar location, burden, transmurality, and mechanical activation curves, target segments are chosen (seen here in white; basal anterior, mid-posterolateral). EDV 1⁄4 end-diastolic volume; EF 1⁄4 ejection fraction; ESV 1⁄4 end-systolic volume; SDI 1⁄4 systolic dyssynchrony using endocardial tracking of CMR cine images in short and long axis. Reproduced with permission from Elsevier due to the creative commons license. Full color available online.
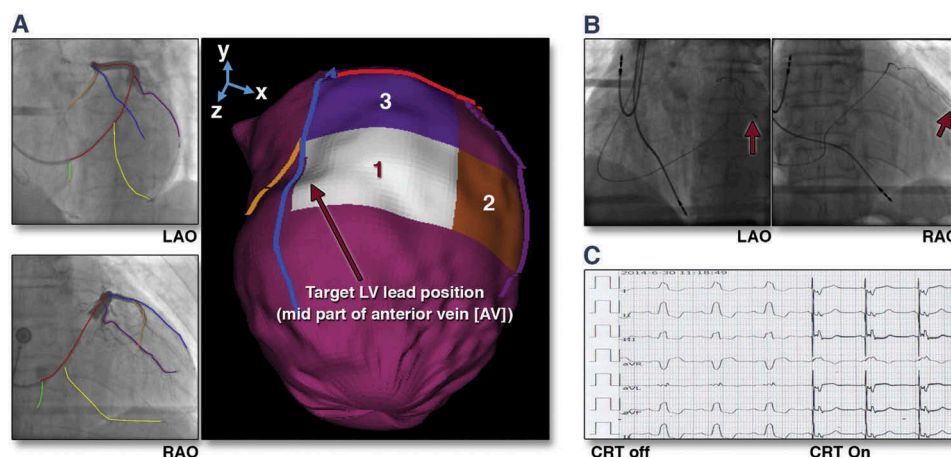

Figure 4. (A) Target venous site for LV lead placement. Major LV veins were drawn on fluoroscopic venograms, reconstructed to a 3D structure, and fused with SPECT LV epicardial surface. The mid part of AV (blue line) was aligned with the optimal segment (white segment), and so was targeted for lead placement. (B) Post-implant fluoroscopy. The LV lead was placed using the guidance in (A). The post-implant images show that the LV lead (red arrows) was on target. (C) Post-implant electrocardiogram. The QRS duration decreased from 168 to 140 ms immediately after the cardiac resynchronization therapy (CRT) device was turned on. RAO 1⁄4 right anterior oblique. Reproduced with permission from Elsevier.

correction. The constraints of the CS anatomy have forced the exploration of novel means or performing resynchronization pacing and of these endocardial CRT holds the most promise. Endocardial LV pacing results in a more physiological, endocardial to epicardial activation pattern, a greater reduction in total LV activation time (LV$_{TAT}$) and an improved hemodynamic performance (greater increases in LV dP/dt$_{max}$) in both the LV [129,146] and RV [147]. It is also associated with a

higher implant success rates, less phrenic nerve stimulation, and far greater access to different pacing sites. The optimal LV endocardial pacing site displays marked inter- and intra-patient variability and while some argue that any endocardial pacing site will invariably prove superior to epicardial stimulation, research has shown that suboptimal BiV$_{ENDO}$ CRT can achieve hemodynamic improvements inferior to those associated with empirically positioned BiV$_{EPI}$ CRT [100]. As such,
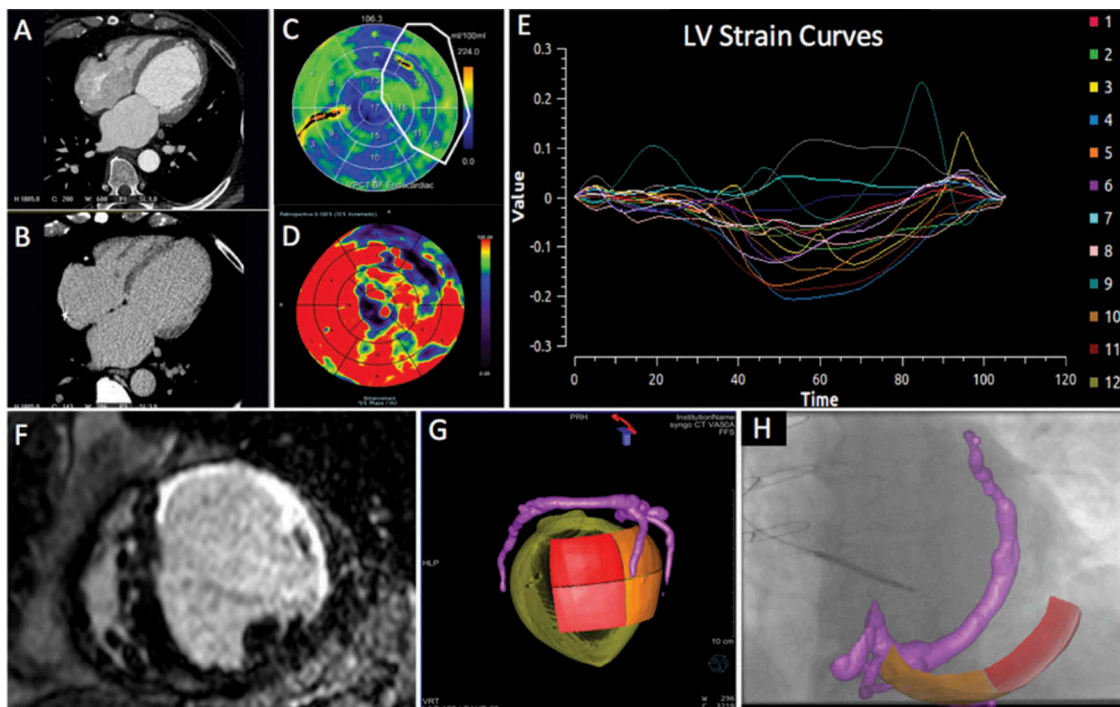
Figure 5. Series of (Dual Energy CT) DECCT-derived scar and image overlay of the coronary sinus and optimal target segment derived from CT strain measurements from one patient: Retrospective CCT demonstrating calcification in a left anterior descending (LAD) and circumflex territory infarct (A). Dual-energy CCT demonstrating subtle ventricular scar in the LAD and circumflex territory (B). Late iodinated enhancement plotted on American Heart Association (AHA) 17-segment bull's-eye plot suggesting scar in the LAD and circumflex territory but also artifact from an existing RV pacing lead in the basal to mid-antero-septum (C). First pass iodine uptake plotted on an AHA 17-segment bull's-eye plot showing what we believe to be residual iodine predominately in the LAD and circumflex territory (D). CCT-derived dyssynchrony curves calculated by myocardial strain (E). Cardiac magnetic resonance short axis image of the mid-LV showing late gadolinium enhancement of the same patient taken 2 years prior to any device implantation for comparison purposes (F). Pre-procedure DECCT-derived coronary sinus segmentation fused with latest mechanical activating segments determined from DECCT-derived strain (G) co-registered and overlaid onto live fluoroscopy using fusion software (H). Reproduced with permission from Oxford University Press.

while endocardial pacing affords the freedom to perform LV stimulation at a customizable location, site selection is even more critical in order to maximize the potential benefits associated with this technique.

Tissue characterization remains an integral parameter when looking to optimize CRT delivery. Targeting viable tissue is clearly beneficial and this can be achieved using a variety of modalities. Undertaking a direct head-to-head comparison of these diagnostic approaches would aid the development of future LV lead guidance systems. While it is clear targeting viable myocardium is beneficial, it remains to be seen precisely how the presence of discrete areas of scar affects the location of the optimal pacing site.

Assessing mechanical dyssynchrony can also be achieved through a variety of modalities;however, the prospective evidence proving dyssynchrony assessments can improve patient selection for CRT is lacking [86,87]. The use of CMR-based dyssynchrony indexes may offer a more reliable solution [18]; however, larger-scale, prospective, randomized validation of these techniques is required before they can be comprehensively endorsed. In the meantime, mechanical dyssynchrony assessments aimed at identifying viable sites exhibiting late mechanical activation do appear to aid LV site selection. It is not clear whether this approach is superior to targeting sites of electrical latency or even whether these two sites are synonymous [112]. Both Q-LV [19] and LVLED [20] appear particularly useful markers to aid site selection. Neither

technique requires sophisticated electroanatomical mapping or additional pre-procedural image processing and instead can be calculated by the operator at the time of LV lead deployment. A more integrated approach is likely to be necessary, however, than simply targeting the site of LEA, particularly in ischemic patients. Instead, the focus should be on targeting a site which displays late activation in the absence of myocardial scar. Narrowing of the paced QRS during pacing appears a less reliable marker of the optimal pacing site, and we would urge caution with this approach given the potential for electromechanical uncoupling. Optimizing the RV pacing site by identifying electrical delay also appears to be beneficial [123], especially when revising a previously implanted system where the position of the LV lead is relatively fixed.

Another novel approach to CRT involves attempting to selectively capture the His-Purkinje network of fast-conducting fibers via LV-only pacing. Rather than trying correct underlying electromechanical dyssynchrony, this approach aims to replicate healthy intrinsic BiV depolarization. New delivery mechanisms allow stimulation of the LV septum via transvenous access [134] meaning this approach may well become increasingly widespread. Whether similar results can be achieved through selective His capture in the RV remains to be seen, although initial studies of this promising pacing modality appear promising [148].

Site selection remains only as good as the adjunctive guidance system given the technical limitations of spatial

orientation using conventional fluoroscopy [138]. Co-registration between 2D and 3D modalities is challenging with the simplest solution integrating pre-implant imaging data with peri-procedural CS balloon venography. However, these systems are unable to determine whether a suitable tributary of the CS subtends the target segment until the procedure has begun highlighting a limitation of the transvenous, epicardial CRT. Guidance systems, which can accurately visualize the entire CS network pre-procedurally, allow decisions to be made regarding not just the most appropriate target but also the most suitable means of targeting this area.

9. Five year view

Transvenous epicardial CRT will continue to function as the default strategy for the delivery of CRT. Pre-procedural imaging and modeling [149] will,however, allow physicians to identify those patients who may benefit from an alternative pacing strategy, either due to a lack of suitable targets or recognition that the target area cannot be accessed via the epicardial coronary venous system. More widespread recognition of cases where this is the case will result in greater use of endocardial pacing, and in particular leadless endocardial pacing systems such as the WiSE-CRT system (WiSE-CRT System, EBR Systems, Sunnyvale, California) which have proved safe and effective and do not require long-term anticoagulation [150]. Growth in endocardial pacing will mandate the increasing use of site selection and guidance given the optimal LV endocardial pacing displays such a high degree of variability.

The WiSE-CRT system has been developed with transfemoral arterial access in mind; however, arterial access complications remain an issue and given the EP community's familiarity with transseptal access, transvenous access [151] will become increasingly derigor. In addition, entire pacing systems will likely become leadless with atrial and right ventricular activation coordinated via communication between the various components.

CMR remains the pre-eminent imaging modality for assessing both tissue characterization and mechanical activation, and the increasing experience with ultrahigh field CMR will inevitably result in improved image quality [152,153]]. Greater spatial resolution will allow detailed visualization of the entire coronary venous tree allowing pre-procedural planning to be performed entirely from one, non-ionizing imaging modality.

Other non-invasive imaging techniques which may become increasingly adopted are ECGI and Holographic imaging systems. ECGI allows an assessment of tissue characterization and can be used to locate areas exhibiting late electrical activation. Refinement of body surface mapping systems now means that instead of multiple electrode vests, a more straightforward ECG belt [154] can derive information on local electrical delay in order to guide LV lead implantation. Holographic imaging systems like the Holoscope (Real View Imaging, Yokneam, Israel) allow users to interact directly with a live 3D digital hologram. Physicians can manipulate the image (rotating, slicing, measuring, and marking) [155] fostering a greater understanding of the patients own unique anatomy.

Key issues

- Transvenous, epicardial CRT remains an excellent therapy for those patients with right substrate and the right anatomy allowing this substrate to be corrected.
- The constraints of CS anatomy have forced the exploration of novel means of performing CRT and of these endocardial CRT holds the most promise.
- Endocardial CRT has several advantages over epicardial CRT, but the optimal endocardial site displays marked variability, and in order to maximize benefits, site selection is critical.
- Assessment of tissue characterization is essential as viable myocardium should always be targeted. This can be achieved in a number of different ways.
- There is conflicting evidence as to whether an assessment of mechanical dyssynchrony can aid in patient selection for CRT over and above current guideline indications, however, targeting sites exhibiting late mechanical activation appears useful.
- Targeting late electrical activation also appears a promising strategy. Q-LV and LVLED appear very useful when looking to identify the optimal site. The site of latest activation is not consistently associated with the optimal hemodynamic improvement. Instead, a position which displays late but not excessively late activation appears the most beneficial.
- Narrowing of the QRS during pacing appears a less reliable marker of the optimal pacing site.
- Optimizing the RV pacing site may be of benefit, especially when revising a previously implanted system where the position of the LV lead is relatively fixed.
- LV-only pacing appears promising, particularly in those with preserved LV function. New delivery technology means both of these systems can be implanted transvenously.
- Site selection is only as good as the adjunctive guidance system. Guidance systems which integrate pre-procedural imaging with peri-procedural CS balloon venography are unable to determine whether a suitable tributary of the CS subtends the target segment until the procedure has begun. This is a limitation of the transvenous epicardial approach. Systems which can directly visualize the CS during pre-procedural planning allow decisions to be made regarding the most suitable method of targeting this area.

Declaration of interest

Reviewer disclosures

Peer reviewers on this manuscript have no relevant financial or other relationships to disclose.

References

Papers of special note have been highlighted as either of interest (•) or of considerable interest (••) to readers.

1. Petersen S, Rayner M, Wolstenholme J. Coronary heart disease statistics: heart failure supplement. Br Hear Found. 2002.
2. Cleland JGF, Daubert JC, Erdmann E, et al. The effect of cardiac resynchronization on morbidity and mortality in heart failure. N Engl J Med. 2005;352:1539–1549.
3. Yu CM, Bleeker GB, Fung JW-H, et al. Left ventricular reverse remodeling but not clinical improvement predicts long-term survival after cardiac resynchronization therapy. Circulation. 2005;112:1580–1586.
4. Mullens W, Grimm RA, Verga T, et al. Insights from a cardiac resynchronization optimization clinic as part of a heart failure disease management program. J Am Coll Cardiol. 2009;53:765–773.
5. Kronborg MB, Johansen JB, Riahi S, et al. An anterior left ventricular lead position is associated with increased mortality and non-response in cardiac resynchronization therapy. Int J Cardiol. 2016;222:157–162.
6. Butter C, Auricchio A, Stellbrink C, et al. Effect of resynchronization therapy stimulation site on the systolic function of heart failure patients. Circulation. 2001;104:3026–3029.
7. Auricchio A, Stellbrink C, Block M, et al. Effect of pacing chamber and atrioventricular delay on acute systolic function of paced patients with congestive heart failure. Circulation. 1999;99:2993–3001.
8. Leyva F, Foley PW, Chalil S, et al. Cardiac resynchronization therapy guided by late gadolinium-enhancement cardiovascular magnetic resonance. J Cardiovasc Magn Reson. 2011;13:29.
   • **This paper confirmed the importance of the practice of targetting viable tissue, characterized using CMR.**
9. Hummel JP, Lindner JR, Belcik JT, et al. Extent of myocardial viability predicts response to biventricular pacing in ischemic cardiomyopathy. Hear. Rhythm. 2005;2:1211–1217.
10. Ypenburg C, Schalij MJ, Bleeker GB, et al. Impact of viability and scar tissue on response to cardiac resynchronization therapy in ischaemic heart failure patients. Eur Heart J. 2006;28:33–41.
11. Huntjens PR, Walmsley J, Ploux S, et al. Influence of left ventricular lead position relative to scar location on response to cardiac resynchronization therapy: a model study. Europace. 2014;16(Suppl 4): iv62–iv68.
12. Ypenburg C, Van Bommel RJ, Delgado V, et al. Optimal left ventricular lead position predicts reverse remodeling and survival after cardiac resynchronization therapy. J Am Coll Cardiol. 2008;52:1402–1409.
13. Khan FZ, Virdee MS, Palmer CR, et al. Targeted left ventricular lead placement to guide cardiac resynchronization therapy: the TARGET study: a randomized, controlled trial. J Am Coll Cardiol. 2012;59:1509–1518.
    •• **This is the first randomized controlled study to demonstrate the benefit of image-guided LV lead placement using speckle-tracking echocardiography.**
14. Döring M, Braunschweig F, Eitel C, et al. Individually tailored left ventricular lead placement: lessons from multimodality integration between three-dimensional echocardiography and coronary sinus angiogram. Europace. 2013;15:718–727.
15. Ansalone G, Giannantoni P, Ricci R, et al. Doppler myocardial imaging to evaluate the effectiveness of pacing sites in patients receiving biventricular pacing. J Am Coll Cardiol. 2002;39:489–499.
16. Saba S, Marek J, Schwartzman D, et al. Echocardiography-guided left ventricular lead placement for cardiac resynchronization therapy results of the speckle tracking assisted resynchronization therapy for electrode region trial. Circ Hear Fail. 2013;6:427–434.

•• **This is the second randomized controlled study to demonstrate the benefit of image-guided LV lead placement using speckle-tracking**
17. Soliman OII, Geleijnse ML. Theuns D MJ, et al. Usefulness of left ventricular systolic dyssynchrony by real-time three-dimensional echocardiography to predict long-term response to cardiac resynchronization therapy. Am. J. Cardiol. 2009;103:1586–1591.
18. Sohal M, Duckett SG, Zhuang X, et al. A prospective evaluation of cardiovascular magnetic resonance measures of dyssynchrony in the prediction of response to cardiac resynchronization therapy. J Cardiovasc Magn Reson. 2014;16:58.
19. Gold MR, Birgersdotter-Green U, Singh JP, et al. The relationship between ventricular electrical delay and left ventricular remodelling with cardiac resynchronization therapy. Eur Heart J. 2011;32:2516–2524.
20. Singh JP, Fan D, Heist EK, et al. Left ventricular lead electrical delay predicts response to cardiac resynchronization therapy. Hear. Rhythm. 2006;3:1285–1292.
    • **This work was the first to confirm the importance of targetting LV tissue which displayed late elctrical activation.**
21. Zanon F, Baracca E, Pastore G, et al. Determination of the longest intrapatient left ventricular electrical delay may predict acute hemodynamic improvement in patients after cardiac resynchronization therapy. Circ Arrhythmia Electrophysiol. 2014;7:377–383.
22. Liang Y, Yu H, Zhou W, et al. Left ventricular lead placement targeted at the latest activated site guided by electrophysiological mapping in coronary sinus branches improves response to cardiac resynchronization therapy. J Cardiovasc Electrophysiol. 2015;26:1333–1339.
23. Rad MM, Blaauw Y, Dinh T, et al. Left ventricular lead placement in the latest activated region guided by coronary venous electroanatomic mapping. Europace. 2014;17:84–93.
24. Foster AH, Gold MR, Mclaughlin JS. Acute hemodynamic effects of atrio-biventricular pacing in humans. Ann Thorac Surg. 1995;59:294–300.
25. Foley PWX, Leyva F, Frenneaux MP. What is treatment success in cardiac resynchronization therapy?. Europace. 2009;11:v58–v65.
26. White HD, Norris RM, Brown MA, et al. Left ventricular end-systolic volume as the major determinant of survival after recovery from myocardial infarction. Circulation. 1987;76:44–51.
27. Picard MH, Young Park M, Altman RK, et al. Clinical Investigations Characteristics of Responders to Cardiac Resynchronization Therapy: The Impact of Echocardiographic Left Ventricular Volume.
28. Spragg DD, Dong J, Fetics BJ, et al. Optimal left ventricular endocardial pacing sites for cardiac resynchronization therapy in patients with ischemic cardiomyopathy. J Am Coll Cardiol. 2010;56:774–781.
29. Derval N, Steendijk P, Gula LJ, et al. Optimizing hemodynamics in heart failure patients by systematic screening of left ventricular pacing sites lateral left ventricular wall coronary sinus are rarely best sites. J Am Coll Cardiol. 2010;55:566–575.
30. Van Gelder BM, Bracke FA, Meijer A, et al. The hemodynamic effect of intrinsic conduction during left ventricular pacing as compared to biventricular pacing. J Am Coll Cardiol. 2005;46:2305–2310.
31. Van Gelder BM, Bracke FA, Meijer A, et al. Effect of optimizing the VV interval on left ventricular contractility in cardiac resynchronization therapy. Am J Cardiol. 2004;93:1500–1503.
32. Steendijk P, Tulner SA, Bax JJ, et al. Hemodynamic effects of long-term cardiac resynchronization therapy: analysis by pressure-volume loops. Circulation. 2006;113:1295–1304.
33. Blanc -J-J, Etienne Y, Gilard M, et al. Evaluation of different ventricular pacing sites in patients with severe heart failure: results of an acute hemodynamic study. Circulation. 1997;96:3273–3277.
34. Duckett SG, Ginks M, Shetty A, et al. Invasive acute hemodynamic response to guide left ventricular lead implantation predicts chronic remodeling in patients undergoing cardiac resynchronization therapy. J Am Coll Cardiol. 2011;58:1128–1136.
    • **This paper was the first to show an acute improvement in AHR of >10% at the time of LV lead implantation was associated with increased likelihood of reverse remodeling.**

35. Rochitte CE, Tassi EM, Shiozaki AA. The emerging role of MRI in the diagnosis and management of cardiomyopathies. Curr Cardiol Rep Current Medicine Group. 2006;44–52.

36. White JA, Patel MR. The role of cardiovascular MRI in heart failure and the cardiomyopathies. Cardiol Clin. 2007;25:71–95.

37. Shehata ML, Turkbey EB, Vogel-Claussen J, et al. Role of cardiac magnetic resonance imaging in assessment of nonischemic cardiomyopathies. Top Magn Reson Imaging. 2008;19:43–57.

38. Sanderson JE, Olsen EGJ, Gatei D. Dilated cardiomyopathy and myocarditis in Kenya: an endomyocardial biopsy study. Int J Cardiol. 1993;41:157–163.

39. Richardson WJW, Clarke SA, Quinn TA, et al. Physiological implications of myocardial scar structure. Compr Physiol. 2015;5:1877–1909.

40. Bogen DK, Rabinowitz SA, Needleman A, et al. An analysis of the mechanical disadvantage of myocardial infarction in the canine left ventricle. Circ Res. 1980;47:728–741.

41. Adelstein EC, Saba S. Scar burden by myocardial perfusion imaging predicts echocardiographic response to cardiac resynchronization therapy in ischemic cardiomyopathy. Am Heart J. 2007;153:105–112.

42. Adelstein EC, Saba S. Baseline scintigraphic abnormalities by myocardial perfusion imaging predict echocardiographic response to cardiac resynchronization therapy in nonischemic cardiomyopathy. Clin Cardiol. 2008;31:217–224.

43. Ypenburg C, Roes SD, Bleeker GB, et al. Effect of total scar burden on contrast-enhanced magnetic resonance imaging on response to cardiac resynchronization therapy. Am J Cardiol. 2007;99:657–660.

44. Ypenburg C, Schalij MJ, Bleeker GB, et al. Extent of viability to predict response to cardiac resynchronization therapy in ischemic heart failure patients. J Nucl Med. 2006;47:1565–1570.

45. Chalil S, Foley PWX, Muyhaldeen SA, et al. Late gadolinium enhancement-cardiovascular magnetic resonance as a predictor of response to cardiac resynchronization therapy in patients with ischaemic cardiomyopathy. Europace. 2007;9:1031–1037.

46. White JA, Yee R, Yuan X, et al. Delayed enhancement magnetic resonance imaging predicts response to cardiac resynchronization therapy in patients with intraventricular dyssynchrony. J Am Coll Cardiol. 2006;48:1953–1960.

47. Kwon DH, Halley CM, Carrigan TP, et al. Extent of left ventricular scar predicts outcomes in ischemic cardiomyopathy patients with significantly reduced systolic function. A delayed hyperenhancement cardiac magnetic resonance study. JACC Cardiovasc. Imaging. 2009;2:34–44.

48. Bleeker GB, Kaandorp TAM, Lamb HJ, et al. Effect of posterolateral scar tissue on clinical and echocardiographic improvement after cardiac resynchronization therapy. Circulation. 2006;113:969–976.

49. Gardner PI, Ursell PC, Fenoglio JJ, et al. Electrophysiologic and anatomic basis for fractionated electrograms recorded from healed myocardial infarcts. Circulation. 1985;72:596–611.

50. Dun W, Baba S, Yagi T, et al. Dynamic remodeling of K+ and Ca2+ currents in cells that survived in the epicardial border zone of canine healed infarcted heart. Am J Physiol Hear Circ Physiol. 2004;287:H1046–H1054.

51. Severs NJ, Bruce AF, Dupont E, et al. Remodelling of gap junctions and connexin expression in diseased myocardium. Cardiovasc Res. 2008;80:9–19.

52. Lambiase PD, Rinaldi CA, Hauck J, et al. Non-contact left ventricular endocardial mapping in cardiac resynchronisation therapy. Heart. 2004;90:44–51.

53. Nayak HM, Verdino RJ, Russo AM, et al. Ventricular tachycardia storm after initiation of biventricular pacing: incidence, clinical characteristics, management, and outcome. J Cardiovasc Electrophysiol. 2008;19:708–715.

54. Shukla G, Chaudhry GM, Orlov M, et al. Potential proarrhythmic effect of biventricular pacing: fact or myth? Hear. Rhythm. 2005;2:951–956.

55. Chalil S, Stegemann B, Muhyaldeen S, et al. Effect of posterolateral left ventricular scar on mortality and morbidity following cardiac resynchronization therapy. Pacing Clin Electrophysiol. 2007;30:1201–1209.

56. Wong JA, Yee R, Stirrat J, et al. Influence of pacing site characteristics on response to cardiac resynchronization therapy. Circ Cardiovasc Imaging. 2013;6:542–550.

57. Kim RJ, Fieno DS, Parrish TB, et al. Relationship of MRI delayed contrast enhancement to irreversible injury, infarct age, and contractile function. circulation. 1999;100:1992–2002.

58. Rasmussen S, Corya BC, Feigenbaum H, et al. Detection of myocardial scar tissue by M-mode echocardiography. Circulation. 1978;57:230–237.

59. Kaandorp TA, Bax JJ, Schuijf JD, et al. Head-to-head comparison between contrast-enhanced magnetic resonance imaging and dobutamine magnetic resonance imaging in men with ischemic cardiomyopathy. Am J Cardiol. 2004;93:1461–1464.

[60] Bakos Z, Ostenfeld E, Markstad H, et al. A comparison between radial strain evaluation by speckle-tracking echocardiography and cardiac magnetic resonance imaging, for assessment of suitable segments for left ventricular lead placement in cardiac resynchronization therapy.

61. Mele D, Nardozza M, Malagù M, et al. Left ventricular lead position guided by parametric strain echocardiography improves response to cardiac resynchronization Therapy. J Am Soc Echocardiogr. 2017;30:1001–1011.

62. Montant P, Chenot F, Goffinet C, et al. Detection and quantification of myocardial scars by contrast-enhanced 3D echocardiography. Circ Cardiovasc Imaging. 2010;3:415–423.

63. Gaibazzi N, Bianconcini M, Marziliano N, et al. Scar detection by pulse-cancellation echocardiography. JACC Cardiovasc Imaging. 2016;9:1239–1251.

64. Winer-Muram HT, Tann M, Aisen AM, et al. Computed tomography demonstration of lipomatous metaplasia of the left ventricle following myocardial infarction. J Comput Assist Tomogr. 2004;28:455–458.

65. Wichmann JL, Bauer RW, Doss M, et al. Diagnostic accuracy of late iodine-enhancement dual-energy computed tomography for the detection of chronic myocardial infarction compared with late gadolinium-enhancement 3-T magnetic resonance imaging. Invest Radiol. 2013;48:851–856.

66. Crean A, Khan SN, Davies LC, et al. Assessment of myocardial scar; comparison between Tc-sestamibi. Clin Med Cardiol. 2009;3:69–763.

67. Peters NS, Wit AL. Myocardial architecture and ventricular arrhythmogenesis. Circulation. 1998;97:1746–1754.

68. Kornowski R, Hong MK, Leon MB. Comparison between left ventricular electromechanical mapping and radionuclide perfusion imaging for detection of myocardial viability. Circulation. 1998;98:1837–1841.

69. Koch KC. vom Dahl J, Wenderdel M, et al. Myocardial viability assessment by endocardial electroanatomic mapping: comparison with metabolic imaging and functional recovery after coronary revascularization. J. Am. Coll. Cardiol. 2001;38:91–98.

70 Perin EC, Silva GV, Sarmento-Leite R, et al. Assessing myocardial viability and infarct transmurality with left ventricular electromechanical mapping in patients with stable coronary artery disease: Validation by delayed-enhancement magnetic resonance imaging. Circulation. 2002;106:957–961.

71. Codreanu A, Odille F, Aliot E, et al. Electroanatomic characterization of post-infarct scars comparison with 3-Dimensional myocardial scar reconstruction based on magnetic resonance imaging. J. Am. Coll. Cardiol. 2008;52:839–842.

72. Wijnmaalen AP. Van Der Geest RJ, Van Huls Van Taxis CFB, et al. Head-to-head comparison of contrast-enhanced magnetic resonance imaging and electroanatomical voltage mapping to assess post-infarct scar characteristics in patients with ventricular tachycardias: real-time image integration and reversed registration. Eur. Heart J. 2011;32:104–114.

73. Desjardins B, Crawford T, Good E, et al. Infarct architecture and characteristics on delayed enhanced magnetic resonance imaging and electroanatomic mapping in patients with postinfarction ventricular arrhythmia. Hear. Rhythm. 2009;6:644–651.

[74] Gornick CC, Adler SW, Pederson B, et al. Validation of a new noncontact catheter system for electroanatomic mapping of left ventricular endocardium. Circulation. 1999;99:829–835.

75. Bhakta D, Miller JM. Principles of electroanatomic mapping. Indian Pacing Electrophysiol J. 2008;8:32–50.

76. Oster HS, Taccardi B, Lux RL, et al. Noninvasive electrocardiographic imaging: reconstruction of epicardial potentials, electrograms, and isochrones and localization of single and multiple electrocardiac events. Circulation. 1997;96:1012–1024.

77. Jmt DB, Janse MJ, Fjl VC, et al. Endocardial mapping by simultaneous recording of endocardial electrograms during cardiac surgery for ventricular aneurysm. J Am Coll Cardiol. 1983;2:947–953.

78. Horowitz LN, Harken AH, Kastor JA, et al. Ventricular resection guided by epicardial and endocardial mapping for treatment of recurrent ventricular tachycardia. NEJM. 1980;302:589–593.

79. Klein H, Karp RB, Kouchoukos NT, et al. Intraoperative electrophysiologic mapping of the ventricles during sinus rhythm in patients with a previous myocardial infarction. Identification Electrophysiologic Substrate Ventricular Arrhythmias Circulation. 1982;66:847–853.

80. Sieniewicz BJ, Panayiotou M, Rashed K, et al. Predicting the optimal site for LV lead deployment using epicardial non-invasive mapping. EP Eur. 2017;19:iii209–iii209.

81. Cuculich PS, Zhang J, Wang Y, et al. The electrophysiological cardiac ventricular substrate in patients after myocardial infarction: noninvasive characterization with electrocardiographic imaging. J Am Coll Cardiol. 2011;58:1893–1902.

82. Liu J, Adelstein E, Saba S. Targeting left ventricular lead placement to improve cardiac resynchronization therapy outcomes. Curr Cardiol Rep. 2013;15:390.

[83] Yu C-M, Fung W-H, Lin H, et al. Predictors of left ventricular reverse remodeling after cardiac resynchronization therapy for heart failure secondary to idiopathic dilated or ischemic cardiomyopathy. Am J Cardiol. 2003;91:684–688.

84. Bax JJ, Bleeker GB, Marwick TH, et al. Left ventricular dyssynchrony predicts response and prognosis after cardiac resynchronization therapy. J Am Coll Cardiol. 2004;44:1834–1840.

85. Suffoletto MS, Dohi K, Cannesson M, et al. Novel speckle-tracking radial strain from routine black-and-white echocardiographic images to quantify dyssynchrony and predict response to cardiac resynchronization therapy. Circulation. 2006;113:960–968.

86. Ruschitzka F, Abraham WT, Singh JP, et al. Cardiac-resynchronization therapy in heart failure with a narrow QRS complex. N Engl J Med. 2013;369:1395–1405.

[87] Chung ES, Leon A, Tavazzi L, et al. Results of the predictors of response to crt (prospect) trial. Circulation. 2008;117:2608–2616.

88. Mele D, Toselli T, Capasso F, et al. Comparison of myocardial deformation and velocity dyssynchrony for identification of responders to cardiac resynchronization therapy. Eur J Heart Fail. 2009;11:391–399.

89. Kapetanakis S, Bhan A, Murgatroyd F, et al. Real-time 3D echo in patient selection for cardiac resynchronization therapy. JACC Cardiovasc Imaging. 2011;4:16–26.

90. Murphy RT, Sigurdsson G, Mulamalla S, et al. Tissue synchronization imaging and optimal left ventricular pacing site in cardiac resynchronization therapy. Am J Cardiol. 2006;97:1615–1621.

91. Becker M, Hoffmann R, Schmitz F, et al. Relation of optimal lead positioning as defined by three-dimensional echocardiography to long-term benefit of cardiac resynchronization. Am J Cardiol. 2007;100:1671–1676.

92. Becker M, Franke A, Breithardt OA, et al. Impact of left ventricular lead position on the efficacy of cardiac resynchronisation therapy: a two-dimensional strain echocardiography study. Heart. 2007;93:1197–1203.

93. Kočková R, Sedláček K, Wichterle D, et al. Cardiac resynchronization therapy guided by cardiac magnetic resonance imaging: a prospective, single-centre randomized study (CMR-CRT). Int J Cardiol. 2018;7:1040–1047.

94. Bilchick KC, Dimaano V, Wu KC, et al. Cardiac magnetic resonance assessment of dyssynchrony and myocardial scar predicts function class improvement following cardiac resynchronization therapy. JACC Cardiovasc Imaging. 2008;1:561–568.

95. Panayiotou M, Mountney P, Brost A, et al. Dynamic mapping of ventricular function from cardiovascular magnetic resonance imaging. 2016 38th Annu. Int. Conf. IEEE Eng. Med. Biol. Soc. IEEE; 2016. p. 4137–4140.

96. Daubert JC, Saxon L, Adamson PB, et al. EHRA/HRS expert consensus statement on cardiac resynchronization therapy in heart failure: implant and follow-up recommendations and management: a registered branch of the European Society of Cardiology (ESC), and the Heart Rhythm Society; and in col. Europace. 2012;2012 (14):1236–1286.

[97] Pourmorteza A, Schuleri KH, Herzka DA, et al. A new method for cardiac computed tomography regional function assessment: stretch quantifier for endocardial engraved zones (SQUEEZ). Circ Cardiovasc Imaging. 2012;5:243–250.

98. Behar JM, Rajani R, Pourmorteza A, et al. Comprehensive use of cardiac computed tomography to guide left ventricular lead placement in cardiac resynchronization therapy. Hear. Rhythm.. 2017;14:1364–1372.

99. Auricchio A, Fantoni C, Regoli F, et al. Characterization of left ventricular activation in patients with heart failure and left bundle-branch block. Circulation. 2004;109:1133–1139.

100. Behar JM, Jackson T, Hyde ER, et al. Optimized left ventricular endocardial stimulation is superior to optimized epicardial stimulation in ischemic patients with poor response to cardiac resynchronization therapy. JACC Clin Electrophysiol. 2016;2:799–809.

   • **This is the first study to demonstrate the superiority of LV endocardial stimulation opposite to a corresponding epicardial position for biventricular pacing.**

101. Ellenbogen KA, Gold MR, Meyer TE, et al. Primary results from the smartdelay determined AV optimization: A comparison to other AV delay methods used in cardiac resynchronization therapy (SMART-AV) trial: A randomized trial comparing empirical, echocardiography-guided, and algorithmic atrioventr. Circulation. 2010;122:2660–2668.

102. Van Gelder BM, Nathoe R, Bracke FA. Haemodynamic evaluation of alternative left ventricular endocardial pacing sites in clinical non-responders to cardiac resynchronisation therapy. Netherlands Hear. J. 2016;24:85–92.

103. Iler MA, Hu T, Ayyagari S, et al. Prognostic Value of Electrocardiographic Measurements Before and After Cardiac Resynchronization Device Implantation in Patients With Heart Failure due to Ischemic or Nonischemic Cardiomyopathy. Am J Cardiol. 2008;101:359–363.

104. Hsing JM, Selzman KA, Leclercq C, et al. Paced left ventricular QRS width and ECG parameters predict outcomes after cardiac resynchronization therapy PROSPECT-ECG substudy. Circ Arrhythmia Electrophysiol. 2011;4:851–857.

105. Bonakdar HR, Jorat MV, Fazelifar AF, et al. Prediction of response to cardiac resynchronization therapy using simple electrocardiographic and echocardiographic tools. Europace. 2009;11:1330–1337.

106. Lecoq G, Leclercq C, Leray E, et al. Clinical and electrocardiographic predictors of a positive response to cardiac resynchronization therapy in advanced heart failure. Eur Heart J. 2005;26:1094–1100.

107. Mollema SA, Bleeker GB, Van Der Wall EE, et al. Usefulness of QRS Duration to Predict Response to Cardiac Resynchronization Therapy in Patients With End-Stage Heart Failure. Am J Cardiol. 2007;100:1665–1670.

108. Ghosh S, Silva JNA, Canham RM, et al. Electrophysiologic substrate and intraventricular left ventricular dyssynchrony in nonischemic heart failure patients undergoing cardiac resynchronization therapy. Heart Rhythm. 2011;8:692–699.

109. Silva JNAA, Ghosh S, Bowman TM, et al. Cardiac resynchronization therapy in pediatric congenital heart disease: insights from noninvasive electrocardiographic imaging. Heart Rhythm. 2009;6:1178–1185.

110. Rodriguez L-M, Timmermans C, Nabar A, et al. Variable patterns of septal activation in patients with left bundle branch block and heart failure. J Cardiovasc Electrophysiol. 2003;14:135–141.

111. Suever JD, Hartlage GR, Magrath RP, et al. Relationship between mechanical dyssynchrony and intra-operative electrical delay times in patients undergoing cardiac resynchronization therapy. J Cardiovasc Magn Reson. 2014;16:4.

112. Fujiwara R, Yoshida A, Fukuzawa K, et al. Discrepancy between electrical and mechanical dyssynchrony in patients with heart failure and an electrical disturbance. PACE Pacing Clin Electrophysiol. 2014;37:576–584.

113. Eschalier R, Ploux S, Lumens J, et al. Detailed analysis of ventricular activation sequences during right ventricular apical pacing and left bundle branch block and the potential implications for cardiac resynchronization therapy. Hear. Rhythm.. 2015;12:137–143.

114. Wilkoff BL, Cook JR, Epstein AE, et al. Dual-chamber pacing or ventricular backup pacing in patients with an implantable defibrillator: the Dual Chamber and VVI Implantable Defibrillator (DAVID) Trial. JAMA. 2002;288:3115–3123.

115. Sharma AD, Rizo-Patron C, Hallstrom AP, et al. Percent right ventricular pacing predicts outcomes in the DAVID trial. Hear. Rhythm.. 2005;2:830–834.

116. De Cock CC, Giudici MC, Twisk JW. Comparison of the haemodynamic effects of right ventricular outflow-tract pacing with right ventricular apex pacing: A quantitative review. Europace. 2003;5:275–278.

117. Fz KHAN, Salahshouri P, Duehmke R, et al. The Impact of the Right Ventricular Lead Position on Response to Cardiac Resynchronization Therapy. Pacing Clin Electrophysiol. 2011;34:467–474.

118. Kutyifa V, Bloch Thomsen PE, Huang DT, et al. Impact of the right ventricular lead position on clinical outcome and on the incidence of ventricular tachyarrhythmias in patients with CRT-D. Hear. Rhythm.. 2013;10:1770–1777.

119. Leclercq C, Sadoul N, Mont L, et al. Comparison of right ventricular septal pacing and right ventricular apical pacing in patients receiving cardiac resynchronization therapy defibrillators: the SEPTAL CRT Study. Eur Heart J. 2016;37:473–483.

120. Derval N, Steendijk P, Gula LJ, et al. Optimizing hemodynamics in heart failure patients by systematic screening of left ventricular pacing sites. J Am Coll Cardiol. 2010;55:566–575.

121. Kumar P, Upadhyay GA, Cavaliere-Ogus C, et al. Right ventricular lead adjustment in cardiac resynchronization therapy and acute hemodynamic response: a pilot study. J Interv Card Electrophysiol. 2013;36:223–231.

122. Sassone B, Gabrieli L, Saccà S, et al. Value of right ventricular-left ventricular interlead electrical delay to predict reverse remodelling in cardiac resynchronization therapy: the INTER-V pilot study. Europace. 2010;12:78–83.

123. Miranda RI, Nault M, Johri A, et al. Maximal electric separation–guidedplacement of right ventricular lead improves responders in cardiacresynchronization defibrillator therapy. Circ Arrhythmia Electrophysiol. 2012;5:927–932.

124. Gasparini M, Bocchiardo M, Lunati M, et al. Comparison of 1-year effects of left ventricular and biventricular pacing in patients with heart failure who have ventricular arrhythmias and left bundle-branch block: the Bi vs Left Ventricular Pacing: an International Pilot Evaluation on Heart Failure P. Am Heart J. 2006;152:155.e1–155.e7.

125. Boriani G, Kranig W, Donal E, et al. A randomized double-blind comparison of biventricular versus left ventricular stimulation for cardiac resynchronization therapy: the Biventricular versus Left Univentricular Pacing with ICD Back-up in Heart Failure Patients (B-LEFT HF) trial. Am Heart J. 2010;159:1052–1058.e1.

126. Thibault B, Ducharme A, Harel FFF, et al. Left ventricular versus simultaneous biventricular pacing in patients with heart failure and a QRS complex ≥120 milliseconds. Circulation. 2011;124:2874–2881.

127. Rao RK, Kumar UN, Schafer J, et al. Reduced ventricular volumes and improved systolic function with cardiac resynchronization therapy: a randomized trial comparing simultaneous biventricular pacing, sequential biventricular pacing, and left ventricular pacing. Circulation. 2007;115:2136–2144.

128. Burns KV, Gage RM, Curtin AE, et al. Left ventricular-only pacing in heart failure patients with normal atrioventricular conduction improves global function and left ventricular regional mechanics compared with biventricular pacing: an adaptive cardiac resynchronization therapy sub-study. Eur J Heart Fail. 2017;19:1335–1343.

129. Hyde ER, Behar JM, Claridge S, et al. Beneficial effect on cardiacresynchronization from left ventricular endocardial pacing is mediated by earlyaccess to high conduction velocity tissue: electrophysiological simulationstudy. Circ Arrhythmia Electrophysiol. 2015;8:1164–1172.

130. Sohal M, Shetty A, Niederer S, et al. Delayed trans-septal activation results in comparable hemodynamic effect of left ventricular and biventricular endocardial pacing insights from electroanatomical mapping. Circ Arrhythmia Electrophysiol. 2014;7:251–258.

131. Sodi-Pallares D, Rodriguez MI, Chait LO, et al. The activation of the interventricular septum. Am Heart J. 1951;41:569–608.

132. Durrer D, Van Dam RT, Freud GE, et al. Total excitation of the isolated human heart. Circulation. 1970;41:899–912.

133. Kavanagh KM, Belenkie I, Duff HJ. Transmural temporospatial left ventricular activation during pacing from different sites: potential implications for optimal pacing. Cardiovasc Res. 2007;77:81–88.

134. Mafi Rad M, Luermans JGLM, Blaauw Y, et al. Feasibility and acute hemodynamiceffect of left ventricular septal pacing by transvenous approach through theinterventricular septum. Circ Arrhythm Electrophysiol. 2016;9:e003344.

135. Rademakers LM, Van HA, Kuiper M, et al. A possible role for pacingthe left ventricular septum in cardiac resynchronization therapy. JACC Clin Electrophysiol. 2016;2:413–422.

136. Bertini M, Mele D, Malagù M, et al. Cardiac resynchronization therapy guided by multimodality cardiac imaging. Eur J Heart Fail. 2016;18:1375–1382.

137. Laksman Z, Yee R, Stirrat J, et al. Model-based navigation of left and right ventricular leads to optimal targets for cardiac resynchronization therapy: a single-center feasibility study. Circ Arrhythmia Electrophysiol. 2014;7:1040–1047.

138. Sommer A, Kronborg MB, Norgaard BL, et al. Left and right ventricular lead positions are imprecisely determined by fluoroscopy in cardiac resynchronization therapy: a comparison with cardiac computed tomography. Europace. 2014;16:1334–1341.

139. Behar JM, Mountney P, Toth D, et al. Real-time X-MRI-guided leftventricular lead implantation for targeted delivery of cardiacresynchronization therapy. JACC Clin Electrophysiol. 2017;3:803–814.

140. Friehling M, Chen J, Saba S, et al. A prospective pilot study toevaluate the relationship between acute change in left ventricular synchronyafter cardiac resynchronization therapy and patient outcome using asingle-injection gated SPECT protocol. Circ Cardiovasc Imaging. 2011;4:532–539.

141. Zhou W, Hou X, Piccinelli M, et al. 3D Fusion of LV venous anatomy on fluoroscopy venograms with epicardial surface on SPECT myocardial perfusion images for guiding CRT LV lead placement. JACC Cardiovasc Imaging. 2014;7:1239–1248.

142. Younger JF, Plein S, Crean A, et al. Visualization of coronary venous anatomy by cardiovascular magnetic resonance. J Cardiovasc Magn Reson. 2009;11:1–8.

143. Sun C, Pan Y, Wang H, et al. Assessment of the coronary venous system using 256-slice computed tomography. Hodgson-Zingman D, Editor. PLoS One. 2014;9:1–7.

144. Zollei L, Grimson E, Norbash A, et al. 2D-3D rigid registration of X-ray fluoroscopy and CT images using mutual information and sparsely sampled histogram estimators. Proc. 2001 IEEE Comput. Soc. Conf. Comput. Vis. Pattern Recognition. CVPR 2001. IEEE Comput. Soc; p. II-696-II-703.

145. Gould J, Behar JM, Rajani R, et al. P333Dual energy cardiac computed tomography to guide cardiac resynchronisation therapy: a feasibility study using coronary venous anatomy, scar and strain to guide optimal left ventricular lead placement. EP Eur. 2018;20:i53–i54.

146. Morgan JM, Biffi M, Gellér L, et al. ALternate Site Cardiac ResYNChronization (ALSYNC): a prospective and multicentre study of left ventricular endocardial pacing for cardiac resynchronization therapy. Eur Heart J. 2016;37:2118–2127.
•• This paper showed the benefit of LV endocardial pacing in a cohort of previous non-responders.

147. Hyde ER, Behar JM, Crozier A, et al. Improvement of right ventricular hemodynamics with left ventricular endocardial pacing during cardiac resynchronization therapy. PACE Pacing Clin Electrophysiol. 2016;39:531–541.

148. Sharma PS, Dandamudi G, Herweg B, et al.Permanent His-bundle pacing as an alternative to biventricular pacing for cardiac resynchronization therapy: A multicenter experience. Hear. Rhythm.. 2018;15:413–420.

149. Lee A, Crozier A, Hyde ER, et al. Biophysical modeling to determine the optimization of left ventricular pacing site and AV/VV delays in the acute and chronic phase of cardiac resynchronization therapy. J Cardiovasc Electrophysiol. 2017;28:208–215.

150. Reddy VY, Miller MA, Neuzil P, et al. Cardiac resynchronization therapy with wireless left ventricular endocardial pacing. J Am Coll Cardiol. 2017;69:2119–2129.

151. Sieniewicz BJ, Gould J, Rimington HMHM, et al. Transseptal delivery of a leadless left ventricular endocardial pacing electrode. JACC: Clin Electrophysiol. 2017;3:1333–1335.

[152] Prothmann M, Von Knobelsdorff-Brenkenhoff F, Töpper A, et al. High spatial resolution cardiovascular magnetic resonance at 7.0 tesla in patients with hypertrophic cardiomyopathy - First experiences: Lesson learned from 7.0 tesla. PLoS One. 2016;11: e0148066.

153. Niendorf T, Schulz-Menger J, Paul K, et al. High field cardiac magnetic resonance imaging: a case for ultrahigh field cardiac magnetic resonance. Circ Cardiovasc Imaging. 2017;10:e005460.

154. Ben JW, Vatterott PJ, Peterson MA, et al. Body surface mapping using an ECG belt to characterize electrical heterogeneity for different left ventricular pacing sites during cardiac resynchronization: relationship with acute hemodynamic improvement. Hear. Rhythm. 2017;14:385–391.

155. Bruckheimer E, Rotschild C, Dagan T, et al. Computer-generated real-time digital holography: first time use in clinical medical imaging. Eur Heart J Cardiovasc Imaging. 2016;17:845–849.